Origin of the Enantioselectivity of Lipases Explained by a Stereo-Sensing Mechanism Operative at the Transition State

Tadashi Ema,* Juka Kobayashi, Soichi Maeno, Takashi Sakai, and Masanori Utaka*

Department of Applied Chemistry, Faculty of Engineering, Okayama University, Tsushima, Okayama 700

(Received August 11, 1997)

The stereoelectronic considerations and the molecular modeling using an X-ray structure of *Rhizomucor miehei* lipase suggested that the lipase-catalyzed reactions proceed under the stereoelectronic control. This suggestion was supported by the semiempirical MO (MNDO-PM3) calculations carried out on the imidazole-catalyzed transesterification as a model reaction. The stereoelectronic effect operates at the transition state (TS) more effectively than at the tetrahedral intermediate (THI). The stabilization energy due to the stereoelectronic effect operating at the TS was estimated to be ca. 5 kcal mol^{-1}. The enantioselectivities for 1-phenylethanol, 1-phenyl-2-propanol, and 1-cyclohexylethanol were estimated in terms of the lipase-induced strain caused at the TS. A TS model generally applicable to chiral secondary alcohols is proposed. The kinetic study supported the TS model. The result that the enantioselectivity in the lipase-catalyzed transesterifications arises from the difference in V_{max} between the two enantiomers rather than from the difference in K_m indicates that the ability of lipases to discriminate between the enantiomers at the TS is high, while the ability to recognize the chirality in the binding step is poor. Furthermore, the difference in V_{max} between the enantiomers was found to result not from the enhanced reactivity of the (*R*)-enantiomers but from the reduced reactivity of the (*S*)-enantiomers.

Among various enzymes, lipases (EC 3.1.1.3) have recently been attracting great interest because of their organic synthetic utility.[1,2] Significant attention should be paid to the high enantioselectivity and broad substrate specificity in the lipase-catalyzed kinetic resolutions of chiral alcohols and the corresponding esters, because the two features are usually difficult to make compatible with each other in other enzymatic reactions. Hence, it is important to disclose the mechanistic aspect of such unique characteristics of lipases. The X-ray crystallographic analyses of several lipases have revealed the following well-conserved structural features: (i) the catalytic triad (Ser–His–Asp (or Glu)) disposed in the top region of the α/β fold, (ii) the oxyanion hole consisting of the peptide backbone NHs, (iii) the lid(s) covering the active site, and (iv) an "oval" binding cleft.[3] The substrate mappings using a broad range of chiral alcohols have also provided useful information on the substrate-binding site of lipases,[4—6] and several active-site models have been proposed.[5] A stereochemical rule for lipases that a large number of chiral secondary alcohols and the corresponding esters obeys has also been reported.[4e,6] The faster-reacting enantiomer is depicted in Chart 1. This empirical rule can provide not only a useful hint to elucidate the mechanistic aspect of the stereoselectivity of lipases but also an index to check the validity of a proposed model.

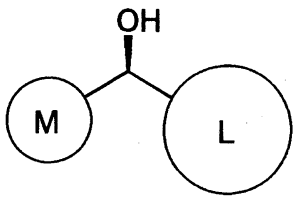

Chart 1. Empirical rule for the lipase-catalyzed kinetic resolutions of racemic secondary alcohols and the corresponding esters. The faster-reacting enantiomer in the lipase-catalyzed enantioselective acylations of secondary alcohols is depicted. The corresponding esters of the enantiomer shown react faster in the lipase-catalyzed hydrolyses. L and M represent the substituents of large and medium sizes, respectively.

The lid that is unique to lipases might regulate the size and shape of the binding pocket to affect the enantioselectivity. However, judging from the diversity of both the secondary structure and the topological arrangement of the lid,[3] the lid should be regarded as a minor factor contributing to the origin of the enantiopreference shown in Chart 1. It is also evident empirically that this enantiopreference (Chart 1) is independent of the direction of the reaction (esterification or hydrolysis).[4e] The inversion of the enantiopreference upon change of the solvent has seldom been reported, although the solvent effect is large in some cases.[7] Therefore, the solvent can also be considered to have a minor effect on the enantioselectivity in comparison with the intrinsic enantiopreference of lipases. The high enantioselectivities of lipases toward a huge number of chiral alcohols so far accumulated are also difficult to explain by the traditional models that depend only on the size, shape and topology of the binding pocket(s); the more the number of specific interactions between lipase and substrates, the more restrictive the substrate specificity, which would be inconsistent with the broad substrate specificity actually observed. Cygler et al. have recently attributed the enantiopreference of lipases and es-

terases (Chart 1) to the spatial arrangement of the catalytic residues on the basis of the X-ray structures.[3f] Because their proposal has been derived from a structural point of view by using a pair of inhibitors, some other significant aspects of the lipase-catalyzed reactions may still remain overlooked.

The above-mentioned considerations prompted us to study the transition state (TS) of the lipase-catalyzed reaction for chiral secondary alcohols. The study of the TS should be essential for a proper understanding of enzymatic *kinetic* behavior. Here we report the theoretical and kinetic study of the lipase-catalyzed transesterifications. We also propose a stereo-sensing mechanism operative at the TS, which is compatible with the high enantioselectivity and broad substrate specificity, and simultaneously which can explain the empirical rule.

Results and Discussion

Application of the Stereoelectronic Theory. Since the stereoelectronic effect originally proposed by Deslongchamps is widely accepted for both nonenzymatic and enzymatic reactions,[8–13] we began our study by applying the stereoelectronic theory to the lipase-catalyzed reaction.

The stereoelectronic theory predicts that the ester C–O bond can be cleaved efficiently if both of the two remaining oxygens of the tetrahedral intermediate (THI) have the lone-pair orbital antiperiplanar to the breaking C–O bond.[8b] Such orbital-assisted breakdowns of the THI of the lipase-catalyzed reaction are illustrated in Scheme 1. We determined the absolute configuration of the THI by the spatial arrangement of the catalytic residues of lipases,[3] in agreement with the proposal of Cygler et al. that the catalytic Ser attacks the *re* face of the ester.[3e,3f] Two possible conformations, g- and a-THI, are shown in Scheme 1; in this paper the prefixes g- and a- designate *gauche* and *anti* conformations, respectively, with respect to the R–O bond of the substrate and the scissile C–O bond on the side of the catalytic Ser. One of the two lone-pair orbitals (meshed orbital) on the Ser O_γ atom should be kept antiperiplanar to the scissile C–O bond on the side of the substrate during the reaction, because the oxyanion must be stabilized by the oxyanion hole.

In the case of the breakdown of g-THI, both of the C–O bonds are allowed to be cleaved, because in each case both of the two remaining oxygens have the lone-pair orbital (shaded or meshed orbitals) antiperiplanar to the breaking C–O bond. In the case of a-THI, the cleavage of the C–O bond on the side of the substrate is stereoelectronically allowed by the same token, whereas the cleavage of the C–O bond on the side of the Ser is stereoelectronically disfavored because only one antiperiplanar lone-pair orbital (shaded orbital) is available (Scheme 1).

Our computer-assisted molecular modeling using the X-ray crystal structure of *Rhizomucor miehei* lipase (RML)[2,3b] indicated that g-THI (R = Me) was generated well without any conformational change of lipase. As for a-THI (R = Me), the methyl group came into conflict with the side chain of Trp 88 of the lid partially covering the active site, which can be avoided by the rotation of the side chain of the Trp.[14] This

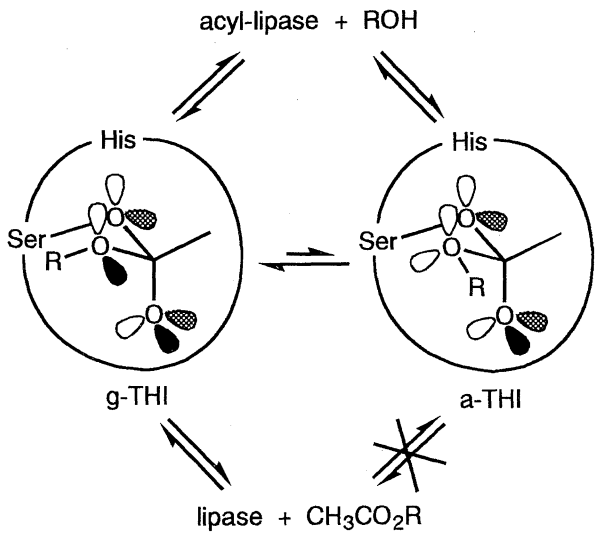

Scheme 1.

result and the stereoelectronic considerations suggest that the lipase-catalyzed reactions proceed via g-THI rather than a-THI. This suggestion was supported by the computational calculations as shown below.

Computational Calculations. (A) Imidazole-Catalyzed Transesterification and Inspection of the Stereoelectronic Effect. We carried out the semiempirical molecular orbital (MO) calculations (the MNDO-PM3 method[15]) on the imidazole-catalyzed transesterification between methyl acetate and methanol (**1**) as a model reaction for the lipase-catalyzed reactions (Scheme 2). The imidazole was located in a manner similar to that of the catalytic His of lipases,[3] and the catalytic Ser is represented by methanol or the methoxy moiety on the left hand of each step in Scheme 2. The carboxylate ion representing the catalytic Asp (or Glu)[16] was not included in our calculations, because the present study focuses not on the magnitude of the activation energy[16] but on the difference in the activation energy between two states (conformers or enantiomers), and because it has not yet been established which mechanism originally proposed for the serine proteases, the "charge-relay mechanism"[17] or the "electrostatic mechanism",[16b,16c,18] is valid for lipases. The model steps corresponding to the formation/collapse of the acyl-enzyme intermediate, which are not relevant to the differentiation of chiral alcohols, are not shown in Scheme 2.

The optimized geometries of g-TS1, g-TS2, and g-THI, together with the single imaginary vibrational frequency for each TS, are shown in Fig. 1. The calculated energies are summarized in Table 1. The imidazole is almost fully protonated at g-TS1 and g-TS2, and each TS resembles methyl acetate being attacked by the methoxide ion; the pyramidalization parameter θ^4 is 22.4° for g-TS1 and 23.1° for g-TS2.[19] The distance between the attacking/leaving methoxide O and the carbonyl C is ca. 1.9 Å, and the protonated imidazole is hydrogen-bonded strongly with the attacking/leaving methoxide O (ca. 1.6 Å) and moderately with the methoxy O of the ester moiety (ca. 1.9 Å). As for g-THI, the parameter θ^4 is 39.5° and the imidazolium ion forms bifurcated hydrogen

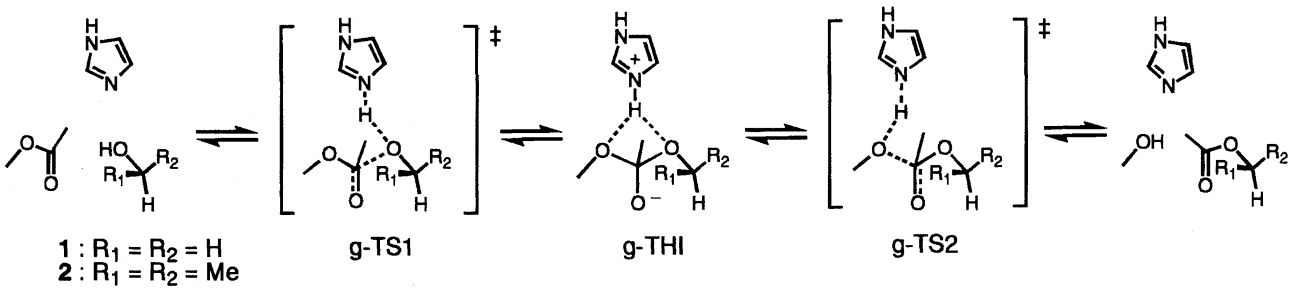

Scheme 2. Only *gauche* conformers are shown for clarity.

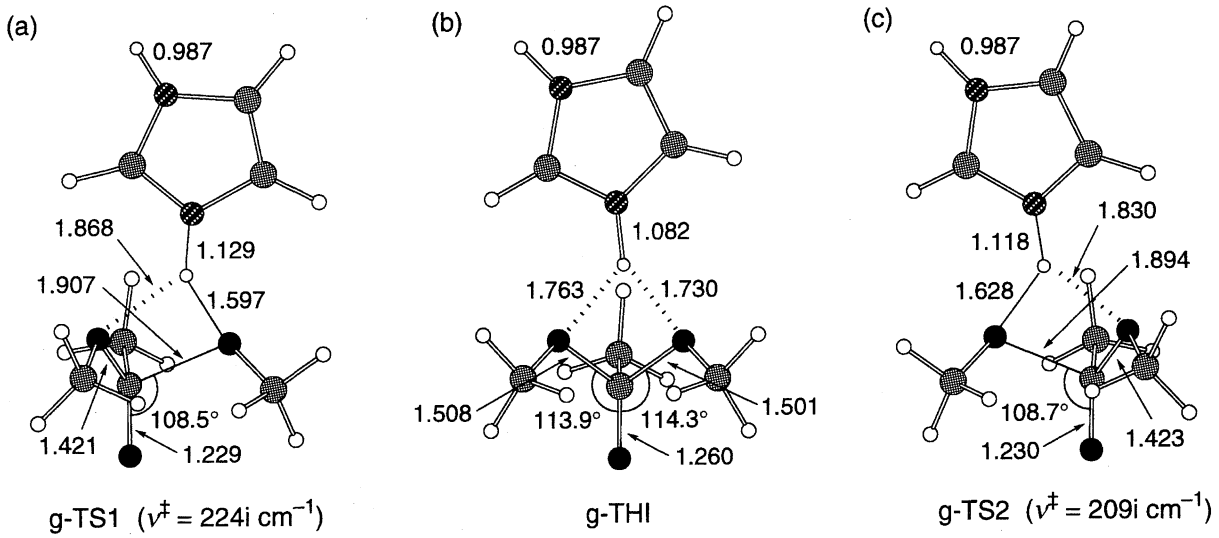

Fig. 1. Optimized geometries of g-TS1, g-TS2, and g-THI of the imidazole-catalyzed transesterification between methyl acetate and methanol (MNDO-PM3). Selected bond lengths in Å.

Table 1. Energies of the *gauche* and *anti* Conformers of THI, TS1, and TS2 Calculated on the Imidazole-Catalyzed Transesterification between Methyl Acetate and Methanol[a)]

	ΔE[b)]	
	gauche	*anti*
THI	46.8	49.2
TS1	49.8	51.0
TS2	49.3	54.4[c)]

a) Calculations performed by the MNDO-PM3 method.[15)]
b) Energy based on the reactants and reported in kcal mol^{-1}.
c) Obtained by the single-point SCF calculation.

bonds equally with the two methoxy Os (ca. 1.7 and 1.8 Å).

The intrinsic reaction coordinate (IRC) calculations started from the g-TS1 or g-TS2 geometry simulated well the expected reaction pathway yielding g-THI or the reactants/products (Scheme 2). Interestingly, in the latter downhill processes the breakdown of each TS was found to consist of the two successive stages: After the proton attached to the imidazole moved to the negatively charged oxygen of the methoxy group, the breaking C–O bond was lengthened. From the principle of the microscopic reversibility, it follows that in the uphill process the neutral alcohol initially attacks the carbonyl group of the ester, followed by the proton transfer from the alcohol O to the imidazole N to reach to the TS, as demonstrated by Kollman et al.[16e)] It is known that the pK_a of the catalytic Ser (pK_a 14) of the serine proteases is far larger than that of the catalytic His (pK_a 6.8) and that the proton transfer should be a high-energy process.[10,11b,18)] It is conceivable that the pK_a of an alcohol, which is attacking the ester as simulated in the present IRC calculations, can be much lower than that of the free alcohol itself and that this type of the reaction sequence (the nucleophilic attack followed by the proton transfer) is a lower-energy pathway to the TS as compared with the reverse counterpart (the proton transfer followed by the nucleophilic attack).[11b,16b,18)] The IRC simulations also indicated that the O=C···O(leaving alcohol) angle changed gradually from ca. 114 to ca. 96° as the C–O bond lengthened from ca. 1.5 to ca. 3.3 Å. This trend is in agreement with a series of crystallographic data.[20)]

Next, we inspected the validity of the stereoelectronic effect[13)] by comparing the energies of g-TS1, g-TS2, and g-THI with those of the corresponding *anti* conformers, a-TS1, a-TS2, and a-THI, respectively. The a-TS1 and a-THI structures were successfully obtained in the same way as that for g-TS1 and g-THI, respectively. On the other hand, several attempts to obtain a-TS2 were unsuccessful, suggesting that a true TS corresponding to a-TS2 may not actually exist. Therefore, the energy of a-TS2 was estimated by the single-point SCF calculation after the appropriate rotation of the

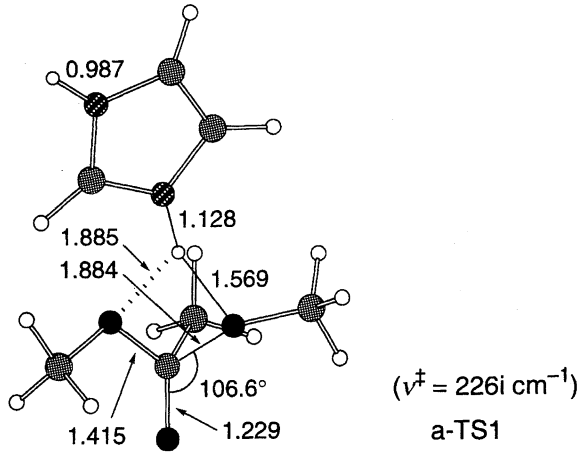

Fig. 2. Optimized geometry of a-TS1 of the imidazole-catalyzed transesterification between methyl acetate and methanol (MNDO-PM3). Selected bond lengths in Å.

dihedral angle around the C–O bond of g-TS2. The results are listed in Table 1, and the optimized a-TS1 geometry is shown in Fig. 2.

The energy difference between a-TS1 and g-TS1 is small (1.2 kcal mol^{-1}), whereas a-TS2 is higher in energy by 5.1 kcal mol^{-1} than g-TS2. It is important to note that these results are consistent with the aforementioned prediction based on the stereoelectronic theory (Scheme 1). The ester-like geometry in g-TS2 (the right-hand moiety in Fig. 1c) appears to maximize the resonance interaction between the lone-pair orbitals having an increased *p* character on the remaining oxygen atoms and the σ^* antibonding orbital of the breaking C–O bond;[9,13] the estimated energy that can be attributed to the stereoelectronic effect (5.1 kcal mol^{-1}) is comparable to the resonance energy of methyl acetate (5.7 kcal mol^{-1}). Therefore, it is reasonable that the stereoelectronic effect operates at the TS more effectively than at the THI (Table 1).[13e]

(B) Chiral Secondary Alcohols. Next, we tried to approach the origin of the enantioselectivity in the lipase-catalyzed reactions for secondary alcohols by means of the computational calculations. In view of the results of the stereoelectronic considerations and the MO calculations, only *gauche* conformers are treated below, unless otherwise noted. Because of both the difficulty in obtaining the TS for complex molecules and the applicability to a variety of secondary alcohols, TS1 and TS2 for 2-propanol (**2**) were obtained in the same way as that for methanol (**1**) (Scheme 1), and then one of the two methyl groups of each TS was replaced by other substituent to generate the chiral alcohol moiety of **3**—**5** in Chart 2. The imidazole moiety was deleted and the internal coordinates of all the carbon and oxygen atoms except the two substituents attached to the chiral carbon were fixed for conformational analysis (B–1) and the docking experiments (B–2).

(B–1) Important Factors in the Enantiomer-Differentiating Process. The conformations of TS1 and TS2 for **3**—**5** were analyzed by the MNDO-PM3 method. The energy maps obtained by rotating the dihedral angle ϕ (shown in Fig. 3a) around the C–O bond of the chiral alcohol moiety by 5° increments revealed that in the lowest-energy conformers the proton attached to the chiral carbon was *syn*-oriented toward the carbonyl O with the dihedral angle ϕ ranging from −29° to +35°. For example, the TS conformers for **3**—**5** whose methyl group attached to the chiral carbon was eclipsed with the carbonyl O were higher in energy by ca. 6—8 and 7—10 kcal mol^{-1} for TS1 and TS2, respectively, than the TS conformers whose proton attached to the chiral carbon was eclipsed with the carbonyl O.[21] As a result, as represented by Fig. 3, in the lowest-energy conformers the larger substituent of the (*R*)- and (*S*)-enantiomers pointed *away from* and *toward* the catalytic imidazole, respectively (for the location of the imidazole, see Fig. 1). Obviously, this fact suggests that the (*S*)-enantiomers have a stronger tendency to disturb the catalytic His and the surrounding hydrogen-bonding network than the (*R*)-enantiomers do (vide infra).

The relative energies ($\Delta E^{\ddagger}_{\text{lowest}}$) of the lowest-energy conformers of the TSs for **3**—**5** are listed in Table 2. It is clear that TS2 is higher in energy than the corresponding TS1 in all cases. The ester moiety in the TS geometry adopts a specific conformation to maximize the stabilization due to the stereoelectronic effect (Fig. 3), and the alkoxy C–O bond of the ester moiety of TS2 (ca. 1.4 Å) is much shorter than the corresponding forming/breaking C–O bond of TS1 (ca. 1.9 Å). As a result, the nonbonded steric repulsions around the substituents attached to the chiral carbon of TS2 become larger than those of TS1. Moreover, it should also be noted that the attacking/leaving chiral alcohol is not restricted by the stereoelectronic requirement at TS1 (Table 1); both of the conformations, g-TS1 and a-TS1, are stereoelectronically allowed, and hence even if g-TS1 is forbidden by severe steric hindrance in the lipase-catalyzed reaction, a-TS1 may be available, suggesting that the enantiomeric discrimination at TS1 is less strict. Accordingly, we propose that TS2 is the rate-determining and enantiomer-differentiating step in the enantioselective lipase-catalyzed reactions.

(B–2) Enantioselectivity Estimated by the Lipase-Induced Strain Energy. The lowest-energy conformations as shown in Fig. 3 correspond to such a situation that lipase is extremely flexible. However, the actual lipase-catalyzed reactions should be accompanied by spatial constraint imposed by the amino acid residues of lipase. Hence, we next tried to estimate the enantioselectivity in terms of the lipase-induced strain caused at the TS.

The lowest-energy conformers of TS1 and TS2 for **3**—**5** were embedded into the X-ray structure of RML,[3b] as follows.[22] The carbon and oxygen atoms of the methoxy group of a TS were superimposed on the C_β and O_γ atoms of the catalytic Ser 144, respectively, and the dihedral angle around this C–O bond was rotated so that the carbonyl oxygen (oxyanion) was fitted into the oxyanion hole; −110° for TS1 and −120° for TS2.[23] The distances between the carbonyl O of the embedded TS moiety and the two backbone Ns of Leu 145 and Ser 82 (oxyanion hole) were 2.8 and 3.1 Å for TS1, 3.1 and 2.8 Å for TS2. These values are close to

Table 2. Enantioselectivities for **3**—**5** Calculated from the Difference in the Energy of the Lipase-Induced Conformers of the TSs between Both Enantiomers.[a]

Alcohol	TS	$\Delta E^{\ddagger}_{\text{lowest}}$ [b]	$\Delta E^{\ddagger}_{\text{ind}}$ [c]	$\Delta\Delta E^{\ddagger}_{\text{ind}}$ [d]	$\Delta\Delta G^{\ddagger}_{\text{expl}}$ [e]
3	TS1(*R*)	0.0	1.7 (1.7)	−1.2[f] (−1.2)	
3	TS1(*S*)	0.7	2.9[f] (2.9)		
3	TS2(*R*)	7.3	9.2 (7.8)	−1.8[f] (−3.2)	−3.4
3	TS2(*S*)	6.3	11.0[f] (11.0)		
4	TS1(*R*)	0.0	1.4 (1.1)	−0.7[f] (−1.0)	
4	TS1(*S*)	−0.7	2.1[f] (2.1)		
4	TS2(*R*)	5.5	9.5 (5.5)	−0.7[f] (−4.7)	−2.9
4	TS2(*S*)	3.8	10.2[f] (10.2)		
5	TS1(*R*)	0.0	2.2 (2.2)	−0.2[f] (−0.2)	
5	TS1(*S*)	−0.3	2.4[f] (2.4)		
5	TS2(*R*)	5.4	11.2 (5.5)	4.0[f] (−1.7)	−2.0
5	TS2(*S*)	3.6	7.2[f] (7.2)		

a) Calculations performed by the MNDO-PM3 method.[15] Energy in kcal mol^{-1}. b) Relative energy for the lowest-energy conformer on the basis of TS1 (*R*). c) Relative energy for the lipase-induced conformer on the basis of TS1 (*R*). Atomic coordinates of RML (entry 4TGL) were used. The values in the parentheses were obtained by using a modified RML, where the side chains of Trp 88 and Leu 258 were rotated to expand the binding cavity (see text). d) Energy difference of the lipase-induced conformers between the (*R*)- and (*S*)-enantiomers. The values in the parentheses were obtained by using a modified RML, where the side chains of Trp 88 and Leu 258 were rotated to expand the binding cavity (see text). e) Calculated from $\Delta\Delta G^{\ddagger}_{\text{expl}}=-RT\ln E$, where the experimental E values were taken from Ref. 6c. f) The criterion of 3.0 Å could not be met. Part of the embedded TS moiety was in unacceptable contact with the side chain(s) of Trp 88 and/or Leu 258.

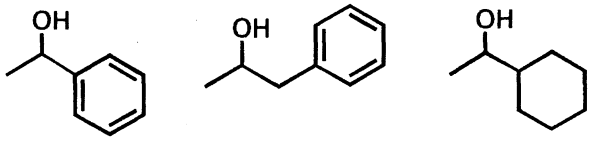

(*R*)- or (*S*)-**3** (*R*)- or (*S*)-**4** (*R*)- or (*S*)-**5**

Chart 2.

those observed in the covalent complex of RML with a TS analog (2.8 and 3.3 Å).[3b] The distances between the alkoxy Os of the embedded TS and the Nε2 of the catalytic His 257 were ca. 3.2—3.6 Å.[22] Next, the other dihedral angles were adjusted to keep the distances between the two substituents and any amino acid residue of lipase more than 3.0 Å.[24] Figures 4 and 5 show the representative lipase-induced TS conformers and TS2 embedded into RML, respectively. Finally, the energies of the lipase-induced TS conformers were obtained by the single-point SCF calculation. The relative energies ($\Delta E^{\ddagger}_{\text{ind}}$) and the calculated enantioselectivities ($\Delta\Delta E^{\ddagger}_{\text{ind}}$) are summarized in Table 2.

The lipase-induced TS conformers for (*R*)-**3** and (*R*)-**4** were calculated to be more stable than the (*S*)-counterparts, in qualitative agreement with the experimental results (Table 2), but the calculated enantioselectivities are underestimated because part of the (*S*)-enantiomers were in unacceptable contact with the side chain(s) of Trp 88 and/or Leu 258. In the case of **5**, the results that the (*S*)-enantiomer did not fulfill the criterion and that the wrong enantiopreference was obtained make the evaluation difficult. Evidently, the binding cavity is somewhat small for these typical substrates **3**—**5**. Therefore, the side chains of Trp 88 and Leu 258 were directed

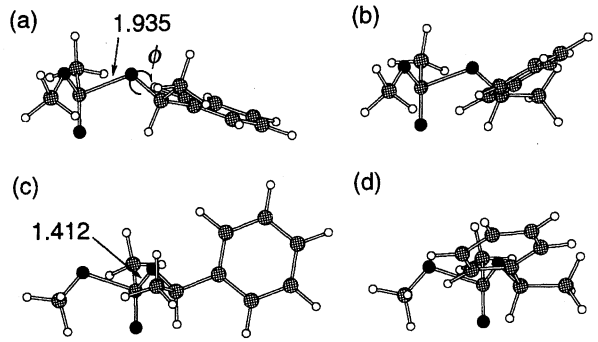

Fig. 3. Lowest-energy conformers of TS1 and TS2 (without the imidazole moiety) for **3** (MNDO-PM3). TS1 for (a) (*R*)-**3** and (b) (*S*)-**3** and TS2 for (c) (*R*)-**3** and (d) (*S*)-**3**. Selected bond lengths in Å.

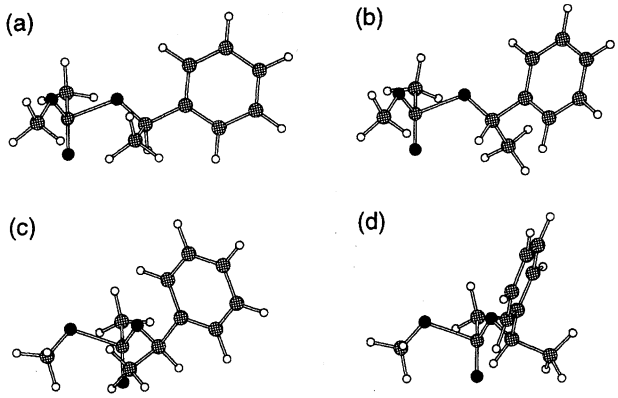

Fig. 4. Lipase-induced conformers of TS1 and TS2 (without the imidazole moiety) for **3** (MNDO-PM3). TS1 for (a) (*R*)-**3** and (b) (*S*)-**3** and TS2 for (c) (*R*)-**3** and (d) (*S*)-**3**.

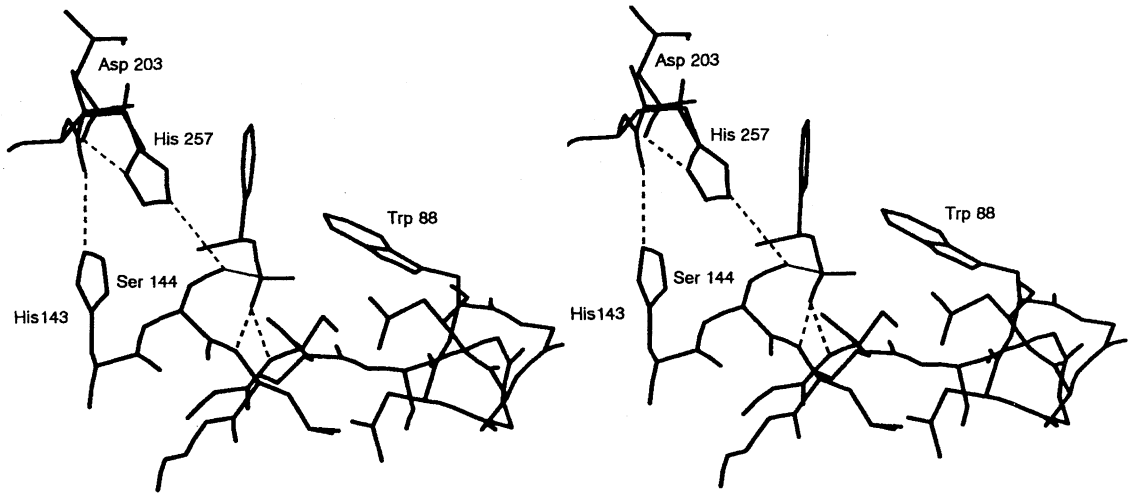

Fig. 5. Stereoview of the active site of RML in which TS2 for (*R*)-**3** is embedded.

outward to expand the binding cavity, because these surface residues seem to fluctuate easily and seem not to seriously damage the catalytic activity. The energies calculated by use of the modified RML are shown in parentheses of Table 2. The enantioselectivities calculated for TS2 are qualitatively consistent with the experimental results (*R*-preference)[6c] in all cases.

The enzyme moiety except the side chains of Trp 88 and Leu 258 is treated as a rigid body in the present calculations, assuming that the strains are caused only in the particular part including the chiral alcohol moiety, and the interactions between the embedded TS moiety and the protein moiety are neglected. Both the appropriate flexibility of the whole lipase and the protein environment as a reaction field[16d] should also be taken into account explicitly in more rigorous calculations.[25] This rigid-body approximation is somewhat inconsistent with the stereo-sensing mechanism described later. Nevertheless, the present primitive method not only afforded successful results for the simple chiral alcohols, suggesting its validity as the first approximation, but also provided useful information to identify the principal origin of the enantioselectivity in the lipase-catalyzed reactions, as summarized below.

General Transition-State Model. Here we propose a TS model to rationalize the enantiopreference of lipases for secondary alcohols (Chart 1). A minimal set of the amino acid residues, which are highly conserved among many lipases and are assumed to be important for the enantioselectivity, is shown in Fig. 6. Although the sequence numbering of RML is used in Fig. 6, the present TS model can hold for many lipases sharing a common structural basis at the active site.[3] It can be seen that the "triangular wall" is formed by Ser 144, His 257, and His 143, and our molecular modeling indicated that the triangular wall plays a significant role in the chiral discrimination at the TS. The detailed size and shape of the binding cavity, which vary with lipase species[3] and can be assumed as a less important factor, are neglected. We employed TS2, because the MO calculations indicated that the most plausible candidate for the enantiomer-differentiating step is TS2 (vide supra). The absolute configuration and the *gauche* conformation of the TS shown in Fig. 6 arise from the spatial arrangement of the catalytic residues and the stereoelectronic effect, respectively (vide supra).

In the case of the faster-reacting (typically, *R* form) enantiomer, the proton attached to the chiral carbon is *syn*-oriented toward the carbonyl O,[21] and the larger substituent (L) attached to the chiral carbon is directed toward the external solvent with small strain (Fig. 6a).[26] The smaller substituent (M) points toward the triangular wall of lipase, which can potentially affect the catalytic activity of lipase.[27] On the other hand, when the larger substituent (L) of the slower-reacting (typically, *S* form) enantiomer is forced to point toward the solvent due to the steric constraint imposed by lipase, the smaller one (M) necessarily causes severe nonbonded repulsion with the carbonyl O (Fig. 6b). When the strain energy is large, the strain should be relieved to some degree by the deformation of the TS geometry. The following three mechanisms are likely to occur, all of which, however, lead to destabilization. (1) If the dihedral angle ϕ_a shown in Fig. 6b is rotated, the directions of the lone-pair orbitals on the alkoxy oxygen will be changed, and as a result, the stabilization due to the stereoelectronic effect will be decreased. (2) If the dihedral angle ϕ_b is rotated, the catalytic His and the surrounding hydrogen-bonding network will be disturbed (vide infra); the MO calculations suggested that the (*S*)-enantiomers have a marked tendency to disturb the catalytic His as compared with the (*R*)-enantiomers (vide supra). (3) If the dihedral angle ϕ_c or ϕ_d is rotated, the oxyanion will be out of the range of the oxyanion hole. The actual stereo-sensing mechanism is probably composed of these factors in varying degrees, depending on the lipase species and the substrate. Thus, the present model focuses on which enantiomer is less favored at the TS; the enantiodifferentiation is assumed to occur because one of the enantiomers is *destabilized* at the TS by unfavorable nonbonded interactions, but not because the other of them gains some additional stabilization factor at the TS, which was demonstrated by our kinetic study (vide infra).

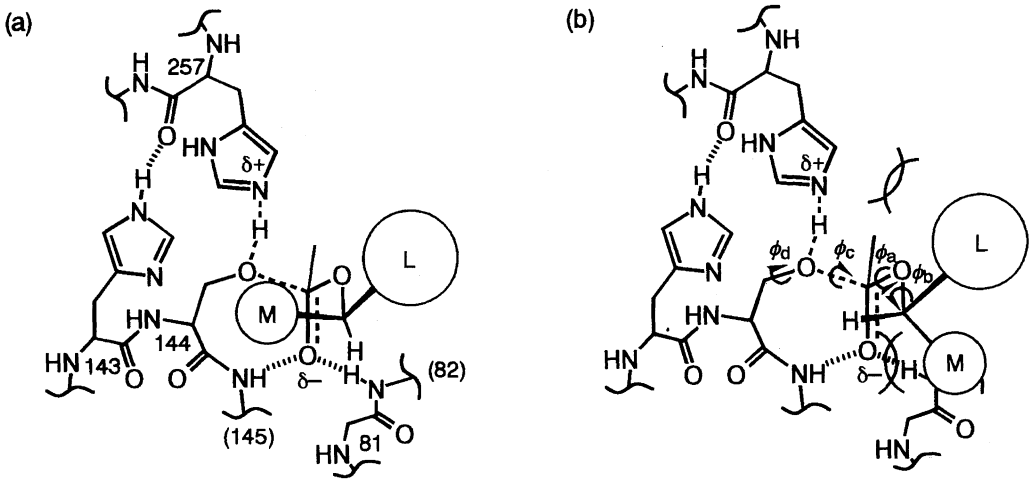

Fig. 6. TS model to rationalize the enantioselectivity of lipases toward chiral secondary alcohols. TS2 is taken as the enantiomer-differentiating step. The electrostatic mechanism is assumed and the catalytic Asp 203 is omitted for clarity. The amino acid residues shown are highly conserved among many lipase species. The "triangular wall" is formed by Ser 144, His 257, and His 143. a) The lipase-induced conformation of the faster-reacting enantiomer. The proton attached to the chiral carbon is *syn*-oriented toward the carbonyl O, and the larger substituent (L) is directed toward the external solvent with small strain. b) The lipase-induced conformation of the slower-reacting enantiomer. The larger one (L) is forced to point toward the solvent, and severe nonbonded repulsion is caused between the smaller one (M) and the carbonyl O. The lipase-induced strain can be reduced by the rotation of the four dihedral angles ϕ_a–ϕ_d, all of which lead to another type of destabilization as described in the text.

Although the space occupied by the smaller substituent (M) of the faster-reacting enantiomer is the bottom part of a single oval cavity that is occupied by the larger one (L) as well, the size of the smaller substituent (M) should be limited,[27] as can be inferred from Figs. 5 and 6a; the single space is dissected by the chiral carbon atom into two spaces to accommodate the substituent (M or L) which differ markedly in size. Therefore, the substrate mappings may have afforded the results as if there was another cavity to accommodate the smaller substituent.[5,6] Figure 6 can also account for the experimental observation that the rigidity adjacent to the chiral center of secondary alcohols is important for high enantioselectivity; e.g., the insertion of one or two methylene groups between the chiral center and the adjacent unsaturated substituent has resulted in a dramatic decrease in the enantioselectivity.[4b,4c,4d,6b] Because the slower-reacting enantiomers of such flexible alcohols can take a conformation to avoid the conflict with the triangular wall, the energy cost for the lipase-induced conformational change becomes small. Thus, the present TS model can rationalize well the general trend; the more unbalanced the bulkiness and/or rigidity of the two substituents attached to the chiral carbon, the higher the enantioselectivity.

It is assumed that the enantioselectivity originates only from the difference in stability of the TS between the two enantiomers. Which enantiomer is bound more tightly or (non)productively[5e] in the binding step (Michaelis complex) is neglected. These assumptions were validated by the experimental results (vide infra). Because the present model does not depend on molecular recognition, it can be applied to a variety of secondary alcohols (broad substrate specificity); the more the number of specific interactions between an enzyme and substrates, the less the number of the substrates to be accepted. The present TS model can also hold for the corresponding esters of secondary alcohols, because it is conceivable that the local TS geometry of the lipase-catalyzed hydrolysis of the ester is similar to that of the lipase-catalyzed acylation of the alcohol even under reaction conditions to which the principle of microscopic reversibility cannot be applied strictly.

Hydrogen Bonds Around the Catalytic Triad Important for the Stereoselectivity. X-Ray structures of lipases indicate that the geometry of the catalytic triad is maintained by the surrounding hydrogen-bonding network.[3] In the case of RML, for example, in addition to the weak hydrogen bond between the catalytic Ser 144 and His 257, the side chain NH of His 143 adjacent to the catalytic Ser is hydrogen-bonded to the backbone C=O of the catalytic His,[3a,3b] forming the triangular wall (Figs. 5 and 6). It is conceivable that steric perturbation on His 143 can be imparted not only to the adjacent catalytic Ser but also to the hydrogen-bonded catalytic His and that the catalytic His itself is likely to be sensitive to steric perturbation because it is commonly located near the protein surface and the C terminus. The amino acid residue located prior to the catalytic Ser is His in most of lipases such as *Pseudomonas* and manmalian lipases.[3a,3b,3c,3h,3i,28] Although it is replaced by Trp in the case of *Candida antarctica* lipase (CAL), the corresponding hydrogen bonding has been observed.[3g] In the case of *Candida rugosa* lipase (CRL) and *Geotrichum candidum* lipase, the corresponding amino acid residue is Glu, which is not hydrogen-bonded with the peptide backbone of the catalytic His exceptionally.[3d,3e,3f,29] The third amino acid residue of the triangular wall may be interesting from the organic synthetic viewpoint; e.g., exceptionally poor or inverted enantioselectivities observed in CRL-mediated kinetic resolutions of a number of alcohols,[6a] which can be resolved normally by other lipases, could be ascribed to the incompleteness of the triangular wall.

Table 3. Kinetic Parameters for the Lipase-Catalyzed Transesterifications of Alcohols **3**—**6** in Diisopropyl Ether[a)]

		V_{max}(M min^{-1} mg(lipase)$^{-1}$)		K_m(M)	
Lipase[b)]	Alcohol	*R*	*S*	*R*	*S*
RML	**3**	$(1.6\pm0.2)\times10^{-4}$	$(3.3\pm0.4)\times10^{-7}$	$(3.5\pm0.6)\times10^{-1}$	$(3.3\pm0.6)\times10^{-1}$
RML	**4**	$(4.6\pm0.9)\times10^{-4}$	$(1.5\pm0.4)\times10^{-7}$	$(2.2\pm0.8)\times10^{-1}$	$(3.2\pm1.4)\times10^{-1}$
RML	**5**	$(3.4\pm0.5)\times10^{-5}$	—[c)]	$(4.8\pm1.1)\times10^{-1}$	—[c)]
RML	**6**	$(6.8\pm2.1)\times10^{-4}$		1.3 ± 0.5	
CAL	**3**	$(1.5\pm0.6)\times10^{-3}$	—[d)]	1.1 ± 0.6	—[d)]
CAL	**4**	$(2.2\pm0.3)\times10^{-4}$	$(8.8\pm1.2)\times10^{-7}$	$(4.8\pm1.2)\times10^{-1}$	$(2.9\pm0.8)\times10^{-1}$
CAL	**5**	$(5.9\pm1.1)\times10^{-4}$	—[d)]	$(1.4\pm0.6)\times10^{-1}$	—[d)]
CAL	**6**	$(1.4\pm0.4)\times10^{-3}$		$(2.2\pm1.3)\times10^{-1}$	
PCL	**3**	$(3.7\pm0.4)\times10^{-5}$	$(6.6\pm0.9)\times10^{-8}$	$(1.0\pm0.2)\times10^{-1}$	$(9.9\pm3.8)\times10^{-2}$
PCL	**4**	$(1.3\pm0.2)\times10^{-5}$	$(3.2\pm0.7)\times10^{-8}$	$(1.4\pm0.4)\times10^{-1}$	$(4.6\pm1.6)\times10^{-1}$
PCL	**5**	$(3.4\pm0.1)\times10^{-5}$	$(3.1\pm0.4)\times10^{-7}$	$(1.4\pm0.1)\times10^{-1}$	$(2.6\pm0.6)\times10^{-1}$
PCL	**6**	$(1.4\pm0.1)\times10^{-4}$		$(1.7\pm0.2)\times10^{-1}$	

a) Conditions: lipase (typically, 3—10 mg and 150—300 mg for (*R*)- and (*S*)-enantiomers, respectively), (optically pure) alcohol (typically, ca. 0.05—0.4 M), vinyl acetate (0.5 M), and three pieces of molecular sieves 4A, dry (i-Pr)$_2$O (2 mL), 30 °C. Because of the heterogeneous reaction, the nonlinear least-squares method was applied to the Michaelis–Menten type of equation: $v_0 = V_{max}(E)_{mg}[S]_0/(K_m+[S]_0)$, where V_{max} is normalized by the weight of lipase $(E)_{mg}$. b) For abbreviations of lipase, see Ref. 2. c) Could not be determined because a saturation relationship was not obtained. Instead, a linear relationship was obtained in the range of 0.05—0.44 M, which is probably due to the weak binding. d) No reaction even in the presence of a large amount (200—300 mg) of lipase.

Bizzozero et al. have suggested that the resistance of dipeptides containing a proline residue to α-chymotrypsin cleavage can be ascribed to the steric hindrance between the methylene groups of the proline ring and the catalytic His during the formation of the THI.[11a)] Cygler et al. have proposed on the basis of X-ray crystallographic analysis that the isopropyl group of (1*S*)-menthyl phosphonate inhibitor covalently linked to the active site of CRL pushes the catalytic His and that this disruption is responsible for the depressed reactivity of the slower-reacting enantiomer of the inhibitor.[3f)] Hirose et al. have demonstrated by means of site-directed mutagenesis that two of the three amino acid residues responsible for the reversal of the enantiopreference of *Pseudomonas cepacia* lipases (PCLs, lipase PS vs. AH) are located in the vicinity of the catalytic His and Asp.[30)] Klibanov et al. have reported that both of the enantiomers of several sterically hindered secondary alcohols are unreactive toward porcine pancreatic lipase.[4a)]

Accordingly, the catalytic triad and the surrounding amino acid residues are important for both enzymatic activity and the stereoselectivity. The general tendency of the (*S*)-enantiomers to sterically disturb the triangular wall of lipases at the TS would lead to their reduced reactivity, which was in fact confirmed by the kinetic study.

Kinetic Study. The kinetic study allows us to gain an insight into the reaction mechanism and to judge the validity of a proposed model. Although the lipase-catalyzed transesterifications in organic solvent is heterogeneous, it is known that reliable parameters can be obtained by fitting the data to the Michaelis–Menten type of equation (see Experimental section).[5e,31a)] Since only several kinetic parameters were available from the literature,[5e,31)] we determined the kinetic parameters for the lipase-catalyzed transesterifications (Scheme 3). We examined various combinations of lipase and the alcohol in order to extract a common origin of the enantioselectivity of lipases. The amino acid sequences of RML, CAL, and PCL used are very different from one another.[3g,28)] Enantiomerically pure alcohols **3**—**5** (Chart 2) and cyclopentanol (**6**) as a reference alcohol having no substituent such as the phenyl and cyclohexyl groups were subjected to the lipase-catalyzed acetylation, and the progress of the reaction was monitored by gas chromatography to obtain the initial rate (v_0). The concentration of the alcohol $[S]_0$ was systematically changed, and the plot of v_0 against $[S]_0$ afforded a typical saturation curve. The apparent V_{max} and K_m values were obtained by the nonlinear least-squares method applied to the Michaelis–Menten type of equation. The results are listed in Table 3. The K_m values may be compared approximately among the different lipase preparations on the assumption that lipases are fully or equally acylated in situ in the presence of a large amount of vinyl acetate. On the other hand, the V_{max} values cannot be compared among the different lipase preparations, because the V_{max} values are normalized by the weight of the lipase powder whose ratio of the enzyme to the inorganic supporting material is different in each case.

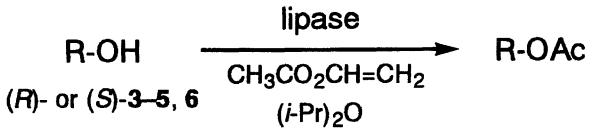

Scheme 3.

Table 3 clearly shows that the enantioselectivity in the lipase-catalyzed transesterifications of **3**—**5** originates from the difference in V_{max} between the enantiomers rather than from that in K_m.[32)] Further comparison of the V_{max} values of

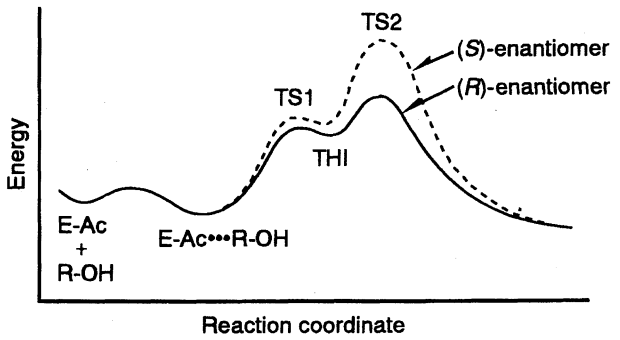

Fig. 7. Energy diagram representing the enantiomer-differentiating step in the lipase-catalyzed acylation of racemic secondary alcohol. E-Ac and R-OH designate the acyl-enzyme intermediate and (*R*)- or (*S*)-alcohol, respectively.

3—**5** with those of **6** reveals that the difference in V_{max} between the enantiomers in turn results not from the enhanced reactivity of the (*R*)-enantiomers but from the reduced reactivity of the (*S*)-enantiomers; e.g., CAL showed no appreciable activity toward (*S*)-**3** and (*S*)-**5**, whereas the V_{max} values for (*R*)-**3** and (*R*)-**5** are comparable to that for **6**. In addition to the small difference in K_m between the enantiomers, the K_m values are relatively large, indicating that the binding of lipases to **3**—**5** in diisopropyl ether is weak; the binding energies calculated from $RT \ln K_m$ are > -1.4 kcal mol^{-1}. Such weak binding is not surprising, because any strong interaction comparable to the hydrophobic interaction in water cannot be expected for **3**—**5** in organic solvents. Importantly, the above features hold for all the appreciable combinations of lipase and the alcohol examined. Accordingly, these experimental results demonstrate that *the chiral discrimination operates at the TS* and that *the ability of lipases to recognize the chirality in the binding step (Michaelis complex) is very poor*, which validates the theoretical basis described above. With the results of the theoretical study as well as the kinetic measurements in mind, the energy diagram is drawn in Fig. 7, representing that the enantioselectivity comes mainly from TS2, neither from TS1 nor from the Michaelis complex, and that the energy difference at TS2 results from the destabilization of the slower-reacting enantiomer.

Conclusions

The present paper has shed light on the origin of the enantioselectivity exerted by lipases from the theoretical and kinetic viewpoints.[33] The MNDO-PM3 calculations carried out on a model reaction indicated that the stereoelectronic effect operating in the ester C–O bond breaking process amounts to ca. 5 kcal mol^{-1} and that the stereoelectronic effect is linked closely to the enantiomer-differentiating step in the lipase-catalyzed reactions; the specific conformation of the TS taken to meet the stereoelectronic requirement leads to the larger destabilization of TS2 in comparison with TS1. The spatial arrangement of the catalytic residues and the stereoelectronic effect determine the absolute configuration and the *gauche* conformation of the TS (specifically, TS2), respectively. As a result, the slower-reacting enantiomers have a tendency to disturb the the catalytic His and the surrounding hydrogen-bonding network and to undergo severe lipase-induced strain at the TS, as compared to the faster-reacting enantiomers.

The merits of the TS model proposed in this paper are the following: (i) The nature of the TS is considered, which should be essential for a proper understanding of the kinetic phenomenon; e.g., its significance is evident from the large difference in V_{max} and negligible difference in K_m between both enantiomers as revealed by the kinetic measurements. (ii) The enantioselectivity in the lipase-catalyzed kinetic resolutions of secondary alcohols can be estimated quantitatively by means of the computational calculations in a relatively simple manner.[33] (iii) Because the present model does not depend on molecular recognition, it can be applied to a wide range of secondary alcohols (broad substrate specificity). (iv) It can explain easily the empirical rule (Chart 1). (v) It will be useful for rationally improving the enantioselectivity in the lipase-mediated kinetic resolutions of secondary alcohols[7d] and for efficiently planning a chemoenzymatic synthetic route. Further studies are necessary to clarify whether the present model can be extended to the cases of chiral primary alcohols and chiral carboxylic acids.

Experimental

Computational Methods. All the MO calculations were performed with MOPAC 94/PM3[15] implemented in the CAChe system (ver. 3.8, Sony/Tektronix). Each TS was searched by using the keyword SADDLE, refined with the keywords TS and PRECISE, and confirmed by the vibrational frequency (FORCE) calculation followed by the IRC simulations. Each structure obtained by the IRC calculations was analyzed by the Visualizer of the CAChe system.

The molecular modeling with lipase was also carried out with the CAChe system. The atomic coordinates of RML (Brookhaven Protein Data Bank entry 4TGL) were used. The orientation of the side chain of His 257 was altered,[22] and the docking experiments were performed without the inhibitor, water molecules, and the hydrogen atoms.

Materials. RML (CHIRAZYME L-9, lyo.) and CAL (CHIRAZYME L-2, carrier-fixed C2, isoform B) provided by Boehringer Mannheim GmbH and PCL (lipase PS, 1% (w/w) powder) provided by Amano Pharmaceutical Co., Ltd. were used without any purification. Vinyl acetate and cyclopentanol commercially obtained were distilled, and dry diisopropyl ether was prepared by distillation from sodium.

Preparations of Enantiomerically Pure Alcohols. Enantiomerically pure alcohols **3**—**5** were prepared by the lipase-mediated kinetic resolutions of racemic alcohols commercially available. The typical procedure is as follows. A heterogeneous solution of PCL (4.0 g), alcohol (23 mmol), and vinyl acetate (46 mmol) in diisopropyl ether (120 mL) was stirred at 450 rpm in a flask with a rubber septum in a thermostat at 30 °C. The progress of the reaction was monitored by TLC, and the reaction was stopped by filtration at an appropriate conversion (typically, 30%). The alcohol and ester were separated by column chromatography, and the latter was hydrolyzed with 10% aq NaOH–MeOH to afford alcohol with high optical purity. The optical purities were checked by capillary gas chromatography (Chrompack, CP-cyclodextrin-β-2,3,6-M-19 column) for **3** and **5** (acetate form), and by HPLC (Daicel, Chiral-

cel OD-H column, hexane : *i*-PrOH = 30 : 1 (v/v)) for **4**. The low optical purity of the remaining alcohol due to the low conversion was improved by the subsequent lipase-catalyzed transesterification (typically, 30% conversion). These procedures were repeated until the optical purity of >99% ee was accomplished for each enantiomer. Enantiomerically pure alcohols **3**—**5** distilled under reduced pressure were used for the kinetic measurements.

Kinetic Measurements. A heterogeneous solution of lipase (typically, 3—10 mg and 150—300 mg for (*R*)- and (*S*)-enantiomers, respectively), (optically pure) alcohol (typically, ca. 0.05—0.4 M), vinyl acetate (0.5 M) (1 M = 1 mol dm^{-3}), and three pieces of molecular sieves 4A in dry diisopropyl ether (2 mL) was stirred at 450 rpm in a test tube with a rubber stopper in a thermostat at 30 °C. At an appropriate time interval, aliquots (50—100 μL) were withdrawn and centrifuged at 6400 rpm for 30 s. The supernatant was analyzed by gas chromatography (PEG column, 3 m) to obtain the conversion (< 15%, calibrated), and five data points were routinely collected to determine the initial rate (v_0) at each substrate concentration $[S]_0$. Plot of v_0 against $[S]_0$ afforded a saturation curve, and the apparent V_{max} and K_m values were obtained by the nonlinear least-squares method applied to the Michaelis–Menten type of equation as follows: $v_0 = V_{max}(E)_{mg}[S]_0/(K_m + [S]_0)$, where V_{max} is normalized by the weight of lipase $(E)_{mg}$.

Supporting Data. Atomic coordinates of the optimized g-TS1, g-TS2, and g-THI geometries for the transesterifications of **1** and **2**, IRC trajectories started from g-TS1 and g-TS2 for **1**, and the $[S]_0$–v_0 plots for (*R*)- and (*S*)-**3**—**5** (17 pages) are deposited as Document No. 71005 at the Office of the Editor of Bull. Chem. Soc. Jpn.

We are grateful to Boehringer Mannheim GmbH and Amano Pharmaceutical Co., Ltd. for providing us with CHIRAZYME L-2,9 and lipase PS, respectively. We also thank Dr. K. Tateno (Boehringer Mannheim GmbH), Dr. J. P. Rasor (Boehringer Mannheim GmbH) and Dr. Y. Hirose (Amano Pharmaceutical Co., Ltd.) for providing useful information about lipases. We are grateful to the SC-NMR Laboratory of Okayama University for the measurement of NMR spectra. This work was financially supported in part by a Grant-in-Aid for Scientific Research from the Ministry of Education, Science and Culture.

References

1) For leading reviews and books, see: a) J. B. Jones, *Tetrahedron*, **42**, 3351 (1986); b) C.-S. Chen and C. J. Sih, *Angew. Chem., Int. Ed. Engl.*, **28**, 695 (1989); c) A. M. Klibanov, *Acc. Chem. Res.*, **23**, 114 (1990); d) "Lipases: Structure, Mechanism and Genetic Engineering," ed by L. Alberghina, R. D. Schmid, and R. Verger, VCH, Weinheim (1991); e) "Preparative Biotransformations: Whole Cell and Isolated Enzymes in Organic Synthesis," ed by S. M. Roberts, K. Wiggins, and G. Casy, John Wiley & Sons, Chichester (1993); f) C.-H. Wong and G. M. Whitesides, "Enzymes in Synthetic Organic Chemistry," Pergamon, Oxford (1994); g) "Enzyme Catalysis in Organic Synthesis," ed by K. Drauz and H. Waldmann, VCH, New York (1994), Vol. 1; h) K. Faber, "Biotransformations in Organic Chemistry," Springer-Verlag, Berlin (1995); i) "Enzymatic Reactions in Organic Media," ed by A. M. P. Koskinen and A. M. Klibanov, Blackie Academic, Glasgow (1996).

2) Abbreviations for the enzymes used in this paper: *Rhizomucor miehei* lipase = RML; *Candida antarctica* lipase (isoform B) = CAL; *Pseudomonas cepacia* lipase = PCL; *Candida rugosa* lipase = CRL; *Humicola lanuginosa* lipase = HLL.

3) For RML, see: a) A. M. Brzozowski, U. Derewenda, Z. S. Derewenda, G. G. Dodson, D. M. Lawson, J. P. Turkenburg, F. Bjorkling, B. Huge-Jensen, S. A. Patkar, and L. Thim, *Nature*, **351**, 491 (1991); b) U. Derewenda, A. M. Brzozowski, D. M. Lawson, and Z. S. Derewenda, *Biochemistry*, **31**, 1532 (1992). For human pancreatic lipase, see: c) F. K. Winkler, A. D'Arcy, and W. Hunziker, *Nature*, **343**, 771 (1990). For *Geotrichum candidum* lipase, see: d) J. D. Schrag, Y. Li, S. Wu, and M. Cygler, *Nature*, **351**, 761 (1991). For CRL, see: e) P. Grochulski, F. Bouthillier, R. J. Kazlauskas, A. N. Serreqi, J. D. Schrag, E. Ziomek, and M. Cygler, *Biochemistry*, **33**, 3494 (1994); f) M. Cygler, P. Grochulski, R. J. Kazlauskas, J. D. Schrag, F. Bouthillier, B. Rubin, A. N. Serreqi, and A. K. Gupta, *J. Am. Chem. Soc.*, **116**, 3180 (1994). For CAL, see: g) J. Uppenberg, M. T. Hansen, S. Patkar, and T. A. Jones, *Structure*, **2**, 293 (1994). For *Pseudomonas glumae* lipase, see: h) M. E. M. Noble, A. Cleasby, L. N. Johnson, M. R. Egmond, and L. G. J. Frenken, *FEBS Lett.*, **331**, 123 (1993). For HLL, see: i) D. M. Lawson, A. M. Brzozowski, S. Rety, C. Verma, and G. G. Dodson, *Protein Eng.*, **7**, 543 (1994).

4) For example: a) G. Kirchner, M. P. Scollar, and A. M. Klibanov, *J. Am. Chem. Soc.*, **107**, 7072 (1985); b) D. Bianchi, P. Cesti, and E. Battistel, *J. Org. Chem.*, **53**, 5531 (1988); c) B. Morgan, A. C. Oehlschlager, and T. M. Stokes, *J. Org. Chem.*, **57**, 3231 (1992); d) J. C. Carretero and E. Domínguez, *J. Org. Chem.*, **57**, 3867 (1992); e) U. Ader, P. Andersch, M. Berger, U. Goergens, R. Seemayer, and M. Schneider, *Pure Appl. Chem.*, **64**, 1165 (1992).

5) a) T. Oberhauser, K. Faber, and H. Griengl, *Tetrahedron*, **45**, 1679 (1989); b) T. Itoh, K. Kuroda, M. Tomosada, and Y. Takagi, *J. Org. Chem.*, **56**, 797 (1991); c) P. G. Hultin and J. B. Jones, *Tetrahedron Lett.*, **33**, 1399 (1992); d) K. Naemura, R. Fukuda, M. Murata, M. Konishi, K. Hirose, and Y. Tobe, *Tetrahedron: Asymmetry*, **6**, 2385 (1995); e) K. Nakamura, M. Kawasaki, and A. Ohno, *Bull. Chem. Soc. Jpn.*, **69**, 1079 (1996).

6) To the best of our knowledge, four groups have independently proposed basically the identical empirical rule in 1991. a) R. J. Kazlauskas, A. N. E. Weissfloch, A. T. Rappaport, and L. A. Cuccia, *J. Org. Chem.*, **56**, 2656 (1991); b) K. Burgess and L. D. Jennings, *J. Am. Chem. Soc.*, **113**, 6129 (1991); c) A. J. M. Janssen, A. J. H. Klunder, and B. Zwanenburg, *Tetrahedron*, **47**, 7645 (1991); d) Z.-F. Xie, *Tetrahedron: Asymmetry*, **2**, 733 (1991).

7) a) P. A. Fitzpatrick and A. M. Klibanov, *J. Am. Chem. Soc.*, **113**, 3166 (1991); b) F. Terradas, M. Teston-Henry, P. A. Fitzpatrick, and A. M. Klibanov, *J. Am. Chem. Soc.*, **115**, 390 (1993); c) B. Herradón, *Synlett*, **1993**, 108; d) T. Ema, S. Maeno, Y. Takaya, T. Sakai, and M. Utaka, *J. Org. Chem.*, **61**, 8610 (1996).

8) a) P. Deslongchamps, "Stereoelectronic Effects in Organic Chemistry," Pergamon Press, Oxford (1983); b) P. Deslongchamps, P. Atlani, D. Fréhel, and A. Malaval, *Can. J. Chem.*, **50**, 3405 (1972); c) P. Deslongchamps, C. Lebreux, and R. Taillefer, *Can. J. Chem.*, **51**, 1665 (1973).

9) a) A. J. Kirby, "The Anomeric Effect and Related Stereoelectronic Effects at Oxygen," Springer-Verlag, Heidelberg (1983); b) A. J. Kirby, *Acc. Chem. Res.*, **17**, 305 (1984); c) A. J. Kirby, "Stereoelectronic Effects," Oxford Univ. Press, Oxford (1996).

10) a) A. Fersht, "Enzyme Structure and Mechanism," 2nd ed, Freeman, New York (1985); b) H. Dugas, "Bioorganic Chemistry: A Chemical Approach to Enzyme Action," 3rd ed, Springer-Verlag, New York (1996).

11) a) S. A. Bizzozero and B. O. Zweifel, *FEBS Lett.*, **59**, 105 (1975); b) S. A. Bizzozero and H. Dutler, *Bioorg. Chem.*, **10**, 46

(1981).

12) a) V. Alphand and R. Furstoss, *J. Org. Chem.*, **57**, 1306 (1992); b) D. R. Kelly, *Tetrahedron: Asymmetry*, **7**, 1149 (1996).

13) For computational calculations regarding the stereoelectronic effect, see: a) S. David, O. Eisenstein, W. J. Hehre, L. Salem, and R. Hoffmann, *J. Am. Chem. Soc.*, **95**, 3806 (1973); b) J.-M. Lehn and G. Wipff, *J. Am. Chem. Soc.*, **96**, 4048 (1974); c) J.-M. Lehn, G. Wipff, and H.-B. Bürgi, *Helv. Chim. Acta*, **57**, 493 (1974); d) D. G. Gorenstein, J. B. Findlay, B. A. Luxon, and D. Kar, *J. Am. Chem. Soc.*, **99**, 3473 (1977); e) K. Taira and D. G. Gorenstein, *Bull. Chem. Soc. Jpn.*, **60**, 3625 (1987).

14) Trp located in a similar position has also been observed in HLL.[3i)]

15) a) J. J. P. Stewart, *J. Comput. Chem.*, **10**, 209 (1989); b) J. J. P. Stewart, *J. Comput. Chem.*, **10**, 221 (1989).

16) a) S. Scheiner, D. A. Kleier, and W. N. Lipscomb, *Proc. Natl. Acad. Sci. U.S.A.*, **72**, 2606 (1975); b) P. A. Kollman and D. M. Hayes, *J. Am. Chem. Soc.*, **103**, 2955 (1981); c) H. Umeyama, S. Nakagawa, and T. Kudo, *J. Mol. Biol.*, **150**, 409 (1981); d) A. Warshel, F. Sussman, and J.-K. Hwang, *J. Mol. Biol.*, **201**, 139 (1988); e) V. Daggett, S. Schröder, and P. Kollman, *J. Am. Chem. Soc.*, **113**, 8926 (1991).

17) D. M. Blow, J. J. Birktoft, and B. S. Hartley, *Nature*, **221**, 337 (1969).

18) In the electrostatic mechanism, the catalytic Asp does not act as a proton acceptor, but stabilizes the imidazolium moiety of the catalytic His electrostatically. L. Polgár and M. L. Bender, *Proc. Natl. Acad. Sci. U.S.A.*, **64**, 1335 (1969). Bender et al. used the term the "general base-general acid catalysis". Here we employ the term the "electrostatic mechanism" used by Umeyama et al.[16c)]

19) The parameter θ^4 defined by Huber et al. is the out-of-plane angle between the C=O bond and the C–C(carbonyl)–O(alkoxy) plane to represent the degree of the pyramidalization of the carbonyl moiety; e.g., θ^4 is 55° for an ideal tetrahedron. R. Huber, D. Kukla, W. Bode, P. Schwager, K. Bartels, J. Deisenhofer, and W. Steigemann, *J. Mol. Biol.*, **89**, 73 (1974).

20) H. B. Bürgi, J. D. Dunitz, and E. Shefter, *J. Am. Chem. Soc.*, **95**, 5065 (1973).

21) This steric and conformational requirement may be relevant to the lack of reactivity of tertiary alcohols and the corresponding esters and may correspond to the smallest pocket proposed by Naemura et al.[5d)] and Nakamura et al.[5e)] to accommodate the proton attached to the chiral carbon. It may also be relevant to the fact that the Gly 81 (Fig. 6) is highly conserved among many lipases.[3)]

22) Because the catalytic His did not appear to be oriented in a way suitable for stabilization of the TSs, probably because of the crystal packing force or the effect of the inhibitor, the dihedral angles of the side chain of His 257 was rotated appropriately; $\chi_1 = 43.7° \rightarrow 55.5°$, $\chi_2 = -90.1° \rightarrow -122.5°$.

23) Derewenda et al. have proposed that the side chain OH of Ser 82 of RML also participates in forming the oxyanion hole.[3a)] However, we did not take Ser 82 OH as part of the oxyanion hole, because it forms a hydrogen bond with the side chain of Asp 91 of the lid (see Fig. 5),[3b)] and because the Ser is not conserved at all.[3)]

24) We first attempted to embed the TSs into RML with the criterion of 3.5 Å, but it was impossible. This difference in the criterion is not crucial qualitatively. The resolution of the X-ray data used is 2.65 Å.[3b)]

25) Molecular mechanics calculations were also carried out for the whole RML in which the TS2 moiety was embedded. Only the two substituents attached to the chiral carbon of the embedded TS2 moiety and the side chains of Trp 88 and Leu 258 were allowed to move, resulting in the amplified enantioselectivities: $\Delta\Delta E^{\ddagger}_{ind}$ in kcal mol^{-1} (substrate) = −22.1 (**3**), −4.1 (**4**), −23.6 (**5**). These enantioselectivities estimated are higher limit, because even a small shift of the atoms which were fixed in our calculations could relax the strain to reduce the enantioselectivity.

26) Most of the glyceride moiety of the natural substrate, triacyl glyceride, is presumably located in the same position as the larger substituent (L) shown in Fig. 6a, and the position of the smaller one (M in Fig. 6a) is occupied by the glyceride methylene H at the TS.[3i)]

27) Figure 6a can explain the high enantioselectivities generally observed for 2-alkanols because the methyl group attached to the chiral carbon of the (*R*)-enantiomers is unlikely to disturb the triangular wall considerably. The experimentally observed trend that as the smaller substituent (M) is more bulky both the enantioselectivity and reactivity are lowered can be explained by the smaller substituent of the (*R*)-enantiomer giving a steric pressure against the triangular wall (see Fig. 6a).

28) a) E. J. Gilbert, *Enzyme Microb. Technol.*, **15**, 634 (1993); b) E. Boel, B. Huge-Jensen, M. Christensen, L. Thim, and N. P. Fiil, *Lipids*, **23**, 701 (1988).

29) This Glu residue, whose side chain CO_2^- points toward the imidazole ring of the catalytic His, may contribute to the electrostatic stabilization of the catalytic His protonated yet to a lesser degree in comparison with Glu of the catalytic triad, in addition to the role suggested by Cygler et al. that the Glu residue expels the carboxylate ion formed by hydrolysis.[3e)]

30) Y. Hirose, K. Kariya, Y. Nakanishi, Y. Kurono, and K. Achiwa, *Tetrahedron Lett.*, **36**, 1063 (1995).

31) a) F. Secundo, S. Riva, and G. Carrea, *Tetrahedron: Asymmetry*, **3**, 267 (1992); b) Y. Okahata, Y. Fujimoto, and K. Ijiro, *J. Org. Chem.*, **60**, 2244 (1995).

32) Similar trends have been reported by other research groups,[5e,31)] and Nakamura et al. have attributed it to the nonproductive (abortive) binding of the slower-reacting enantiomers.[5e)]

33) For other approaches to understand the factors determining the stereoselectivity of hydrolytic enzymes, see: a) M. Norin, K. Hult, A. Mattson, and T. Norin, *Biocatalysis*, **7**, 131 (1993); b) T. Lee and J. B. Jones, *J. Am. Chem. Soc.*, **118**, 502 (1996); c) V. Martichonok and J. B. Jones, *J. Am. Chem. Soc.*, **118**, 950 (1996); d) T. Ke, C. R. Wescott, and A. M. Klibanov, *J. Am. Chem. Soc.*, **118**, 3366 (1996).